



Lebanese American University Repository (LAUR)

Post-print version/Author Accepted Manuscript

Publication metadata

Title: Effect of the number of broken wire wraps on the structural performance of PCCP with full interaction at the gasket joint

Author(s): Masood Hajali, Ali Alavinasab and Caesar Abi Shdid

Journal: Journal of Pipeline Systems Engineering and Practice

DOI/Link: [https://doi.org/10.1061/\(ASCE\)PS.1949-1204.0000219](https://doi.org/10.1061/(ASCE)PS.1949-1204.0000219)

How to cite this post-print from LAUR:

Hajali, M., Alavinasab, A., & Shdid, C. A. (2015). Effect of the Number of Broken Wire Wraps on the Structural Performance of PCCP with Full Interaction at the Gasket Joint. *Journal of Pipeline Systems Engineering and Practice*. Doi: 10.1061/(ASCE)PS.1949-1204.0000219

© 2015

This Open Access post-print is licensed under a Creative Commons Attribution-Non Commercial-No Derivatives (CC-BY-NC-ND 4.0)



This paper is posted at LAU Repository

For more information, please contact: archives@lau.edu.lb

1 **Effect of the Number of Broken Wire Wraps on the Structural Performance of PCCP with**
2 **Full Interaction at the Gasket Joint**

3 Masood Hajali, P.E., M. ASCE¹, Ali Alavinasab, P.E., M. ASCE^{2*}, Caesar Abi Shdid, P.E., M.
4 ASCE³

5
6 **Abstract:** Broken prestressing wire wraps are the main cause of failure in prestressed concrete
7 cylinder pipes (PCCP). The effect of the number and location of broken wire wraps on the
8 structural performance of PCCP is investigated using advanced numerical modeling that
9 considers full interaction between the spigot and bell ends of adjacent pipes. The stresses and
10 strains in the various components of PCCP are evaluated with increasing internal pressure. A
11 sensitivity analysis is performed to understand how manipulating the severity of the damage
12 through varying the number of broken wire wraps affects the internal fluid pressure that causes
13 failure. A 244 cm (96-inch) embedded cylinder pipe (ECP) is modeled with 5, 35, 70, and 100
14 broken wire wraps. The results obtained show that the internal fluid pressure required to cause
15 failure can be as much as 14% lower when the damage is at the joint, and that the internal
16 pressure that causes yielding of the wire wraps decreases about 65% as the severity of the
17 damage increases from 5 to 100 broken wires.

18 **CE Database Subject Headings:** Concrete Pipes; Pipe Joints; Prestressed concrete cylinder
19 pipes; Numerical Analysis; Earth Pressure; Water Pressure; Finite Element Method.

20 **Introduction**

¹ Ph.D., Structural Engineer, Pure Technologies, 3040 State Route 22 West, Suite 130, Branchburg, NJ 08876

² Ph.D., Senior Structural Engineer, Pure Technologies, 3040 State Route 22 West, Suite 130, Branchburg, NJ 08876

Tel: +1(908)526-6600, Email: ali.alavinasab@puretechltd.com

*Corresponding author

³ Ph.D., Assistant Professor, Lebanese American University, Department of Civil Engineering, 211 E 46th St., New York, NY 10017, USA

21 Prestressed Concrete Cylinder Pipe (PCCP) was first manufactured in 1942 as Lined
22 Cylinder Pipe (LCP). Another type of PCCP, known as Embedded Cylinder Pipe (ECP), was
23 developed in 1952 and had concrete encasement of the steel cylinder on both sides and
24 prestressing wire wrapped around the outer concrete core. The design and manufacturing
25 standards of PCCP in the United States were gradually developed beginning in 1943, with the
26 first tentative consensus standard for PCCP being approved by the American Water Works
27 Association (AWWA) in 1949. The AWWA C301 *Standard Specifications for Reinforced*
28 *Concrete Water Pipe - Steel Cylinder Type, Prestressed* (AWWA C301-52) was revised multiple
29 times, with the latest revision being released in 2007 (AWWA C304-2007).

30 PCCP consists of a concrete core, a steel cylinder, high tensile prestressing wires, and an
31 outer mortar coating layer. The concrete core is the structural load-bearing component with the
32 steel cylinder acting as a water barrier between inner and outer core concrete layers. The
33 prestressing wire is an important component of the PCCP that produces a uniform
34 circumferential compressive stress in the concrete core that offsets tensile stresses in the pipe.
35 The mortar coating protects the prestressing wires from physical damage and external corrosion.
36 Rupture of prestressing wires around the concrete core can be the result of damage due to
37 unnoticed installation damage, post-installation excavation damage, corrosion, hydrogen
38 embrittlement, overloading, or manufacturing defects. As a result of this loss of circumferential
39 compressive stress around the pipe, tensile stresses will develop that can lead to cracking of the
40 concrete core and cause leakage or damage in the pipe.

41 While ultrasonic tomography methods—such as the one described by Abi Shdid and Hajali
42 (2014)—and direct inspection by robotic equipment can detect damage, they can be prohibitively
43 expensive. Other available, and similarly expensive to use, methods are: zoom camera,

44 electroscanning, digital scanning, laser profiling, and sonar (Selvakumar et al. 2013). Some
45 researchers have attempted to solve this by proposing quantitative methods to judge if a concrete
46 pipe displays corrosion, cracks, or breakage. He and Koizumi (2012) proposed such
47 quantification method that is based on various pipe factors, including pipe diameter, number of
48 years since installation, type of road and foundation, overburden, and pipe slope. However, such
49 quantification methods can only predict the likely extent of damage to an existing sewage pipe
50 system, and fall short of an accurate modeling of the damage based on internal and external
51 loads. Thus, numerical modeling remains to be the most efficient method available to analyze
52 and assess the structural condition of PCCP.

53 **Background**

54 The knowledge surrounding the behavior of PCCP under combined internal and external
55 loading has been gradually amassed since the mid-1950s, and the various investigations into
56 PCCP failures have led to the evolution of the design standards to follow PCCP failures. Despite
57 the significant improvements in the design and manufacturing of PCCP, the inclusive
58 understanding of the structural behavior and performance of damaged PCCP is still under
59 investigation. Xiong et al. (2010) used a nonlinear FEM to study the correlation between the
60 degree of prestressing stresses during manufacturing of PCCP and their associated resultant
61 stresses in the concrete core and prestressing wires. The study also compared the resultant stress
62 obtained with another FEM model that replaces the effects of tensile stresses in prestressing
63 wires with an equivalent radial pressure around the pipe. The results obtained from the
64 equivalent radial pressure model were within a 10% deviation of the proposed model (Xiong et
65 al. 2010).

66 Rauniyar (2013) performed full-scale experimental tests as well as numerical modeling of
67 ECP under three-edge bearing conditions. The study utilized three-dimensional nonlinear finite
68 element analysis for the numerical modeling, and used composite material with complex stress
69 phenomenon due to prestress and interaction between the various component layers of the ECP.
70 The model accounted for the contribution of each component, the manufacturing process, and the
71 simultaneous effects of shrinkage, creep and relaxation (Rauniyar 2013). More advanced models
72 have been used in recent studies to investigate the behavior of PCCP using an extended form of
73 the finite element method (XFEM). Alavinasab et al. (2011a) used XFEM to study crack
74 initiation, growth, and life prediction analysis of damage in Prestressed Concrete Noncylinder
75 Pipe (NCP). Nonlinear FEM has been used not only in static analysis of PCCP, but also in the
76 dynamic response of PCCP. Alavinasab et al. (2010, 2011b) used FEM to evaluate the natural
77 frequencies and mode shapes for Structural Health Monitoring (SHM) of PCCP.

78 Najafi et al. (2011) proposed an appropriately designed rolled groove joint that could be
79 incorporated into AWWA C303 bar-wrapped concrete pressure pipe. The study used three-
80 dimensional nonlinear numerical finite element modeling, analysis and design optimization to
81 arrive at a viable joint with an optimal stab depth and appropriate rodwrap termination design in
82 both the bell and spigot to provide sufficient stiffness. Experimental results from full-scale testing
83 of rolled groove joint incorporated into a bar-wrapped concrete pressure pipe manufactured to
84 AWWA standard C303 specifications were presented that showed that pipes with such joints can
85 sustain transient internal pressures in excess of 2 MPa without displaying any signs of joint
86 leakage or pipe deformation (Najafi et al. 2011).

87 Wilson (2011) presented a general analysis using a mathematical model for the failure of a
88 buried steel pipeline under simultaneous hoop tension and transverse loading. The developed

89 model is based on classical energy and beam theories. The model was validated using a case
90 study where such tensile and transverse loads on a buried pipe were developed from pipe
91 undermining due to an adjacent excavation collapse (Wilson 2011). Coghill (2013) presented an
92 example decision-making tool used by the Asset Management Program team at the San Diego
93 County Water Authority used to ensure the continued safe and reliable water supply to its
94 customers. The study examined the factors that require consideration when rehabilitating PCCP
95 (Coghill 2013).

96 The structural performance of damaged PCCP is not only dependent on the number of
97 broken prestressing wire wraps, but also on the location of the break regions along the length of
98 the pipe. Alavinasab et al. (2013) studied the effect of the location of broken wire wraps on the
99 strength of PCCP using advanced computational modeling. The study compared three different
100 locations for the defect: at the spigot joint, at the bell joint, and in the barrel of the pipe. The
101 study did not however consider the interaction between the bell end and spigot end of the pipe.
102 The results found that the strength reduction for a low to medium number of wire wrap breaks at
103 a joint was about 20%, and the study concluded that cracking in the pipe will occur at lower
104 pressure when the defects occurred at the joint rather than in the middle of the pipe. Alavinasab
105 and Hajali (2014) studied the effects of broken wire wraps at the joint in the safe operation of an
106 adjacent pipe.

107 Nasser and Saleh (2008) developed a PCCP wire breaks prediction model using Artificial
108 Neural Networks trained on real-world acoustic monitoring data. The developed model takes as
109 input: the monitoring period, pipe age, soil resistivity, design pressure, design soil density,
110 design soil cover, type of pre-stressing wire wrap, wire diameter, and wire pitch; and predicts the
111 number of wire breaks as an output (Nasser and Saleh 2008). Another approach was developed

112 by Kleiner et. al.(2004) to model the deterioration of buried PCCP using a fuzzy rule-based, non-
113 homogeneous Markov process. The model yielded possibility of failure at every point along the
114 life of the pipe. However, adequate and sufficient data to validate the model were not provided
115 (Kleiner et. al. 2004).

116 **Problem Statement and Main Contribution**

117 ***PCCP Joints***

118 The rigid construction of PCCP makes the joint an important component of the pipe
119 system. The function of a pipeline generally determines the performance requirements of the
120 joints. In addition to making installation easier, joints are designed so that when sections are laid
121 together they will make a continuous line of pipe with an interior free from irregularities. Joints
122 are normally designed to provide soil-tightness, water-tightness, the ability to accommodate
123 lateral and longitudinal movement, and the strength to handle shear that causes vertical
124 movement.

125 Joints in PCCP consist of a spigot ring, a bell ring, a rubber gasket, and grout on the
126 exterior of the joint between the two pipes. Spigot and bell rings are welded to each end of the
127 steel cylinder. Joints are designed to allow a pipe to deflect during installation and operation
128 while maintaining a watertight seal. Rubber gaskets are used between the steel rings to facilitate
129 both flexibility and the sealing of the joint. When joined, the bell and spigot ends compress the
130 rubber gasket into a groove to form a high pressure seal as shown in Figure 1. Such a joint
131 provides high shear strength, excellent water tightness, and flexibility. A layer of mortar or
132 cement paste is placed on the inner side of the bell ring and on the external side of the spigot end

133 of the pipe. The exterior of the joints are subsequently grouted to protect the steel joint rings
134 from deterioration.

135 Figure 1. Schematic of the joint in PCCP

136

137 ***Theoretical and Practical Motivation***

138 Once over tensioned, concrete begins to crack and its load carrying capacity decreases with
139 additional strain. At high tensile strains, the load carrying capacity of the concrete core becomes
140 negligible, and the loads are transferred through other components of the PCCP. This load
141 transformation differs at the joints due to the interaction between the pipe's spigot ring, rubber
142 gasket, and bell ring. The interaction between adjacent pipes thus affects the performance of
143 PCCP.

144 The effects of the location of broken prestressing wire wraps on the performance of
145 damaged PCCP has not been thoroughly investigated, and the few studies available in the
146 literature have not considered the effect of the interaction at the joints between adjacent pipes
147 when investigating the relationship between the location of broken wire wraps and the failure
148 pressure of PCCP. Broken wire wraps in PCCP can occur near the joint or in the barrel (middle)
149 of the pipe, as shown in Figure 2. The objective of this study is to investigate how the location of
150 wire wrap breaks affects the strength of the PCCP while considering full interaction between the
151 bell and spigot ends of the adjacent pipes. Such understanding is critical to owners and inspectors
152 in evaluating both the short- and long-term performance of a pipeline system.

153 **Approach**

154 Evaluating the structural performance of a damaged PCCP at a joint is a complex nonlinear
155 problem due to the interaction between not only the broken prestressing wire wraps and the end
156 of the pipe, but also because of the relative displacement and rotation between adjacent pipes. A
157 244 cm (96-inch) ECP was considered and modeled for this purpose, and the stresses and strains
158 developed in the prestressing wire wraps, concrete core, and steel cylinder were compared for the
159 cases of wire breaks at the joint and in the middle of the pipe. The structural performance of the
160 PCCP was evaluated using four (4) different measurements: micro cracking, visible cracking,
161 yielding of wire wraps, and rupture stress of wire wraps.

162 Figure 2. Broken wire wraps at different locations in PCCP

163

164 ***Finite Element Modeling***

165 A numerical model of a 244 cm (96-inch) diameter Class 125-14 ECP with a length of 6.1
166 m (20 feet) is constructed using three-dimensional nonlinear finite elements with consideration
167 given to the manufacturing process in order to incorporate the creep and shrinkage effects of the
168 concrete. The ECP section is modeled using a composite element with five (5) layers
169 representing the inner concrete core, the steel cylinder, the outer concrete core, the prestressing
170 wire, and the mortar coating. Care is taken when modeling the prestressing wire wraps and the
171 joint rings to ensure that a realistic behavior of the ECP was achieved. The model predicts the
172 performance of a PCCP, utilizing the tensile strengths of the prestressing wire, the steel cylinder,
173 and the concrete core, as well as a plasticity algorithm that simulates concrete crushing in
174 compression regions. The model assumes perfect interface between the prestressing wires and
175 the concrete. A four-node quadratic shell element, in which each node has six degrees of

176 freedom, is used in modeling the undamaged and damaged portions of the pipe. An eight-node
177 linear brick element, in which each node has three translational degrees of freedom, is used for
178 modeling the joint ends of the pipe. The finite element model of the bell end of the pipe is shown
179 in Figure 3.

180 Figure 3. Spigot and bell ends of the PCCP numerical model

181
182 The ECP section was modeled based on the tensile strength of concrete and a plasticity
183 algorithm that facilitated concrete crushing in compression regions. The concrete was modeled
184 using a three-dimensional composite axi-symmetric element with additional adjustments made to
185 predict the failure of brittle materials. Cracking and crushing were determined by a failure
186 surface, which formed the boundary between the undamaged zone and failure (damaged) zone.
187 Once the failure surface was reached, cracking or crushing occurred. The nonlinear plastic-
188 damage behavior of concrete, Lubliner et al. (1989) and Lee and Fenves (1998), is defined by
189 the multi-linear stress-strain relationships governed by scalar damaged elasticity as shown in
190 Equations 1 and 2 (Hajali and Abi Shdid (2013)).

$$191 \quad \sigma = D^{el} : (\varepsilon - \varepsilon^{pl}) \quad (1)$$

$$192 \quad D^{el} = (1 - d)D_0^{el} \quad (2)$$

193 where D_0^{el} is the initial (undamaged) elastic stiffness of the material, D^{el} is the degraded elastic
194 stiffness, and d is the scalar stiffness degradation variable, which can take values from zero
195 (undamaged material) to one (fully damaged material). Damage associated with the failure

196 mechanisms of the concrete (cracking and crushing) therefore results in a reduction in the elastic
197 stiffness.

198
$$\dot{\epsilon} = \dot{\epsilon}^{el} + \dot{\epsilon}^{pl} \quad (3)$$

199 where $\dot{\epsilon}$ is the total strain rate, $\dot{\epsilon}^{el}$ is the elastic component of the strain rate, and $\dot{\epsilon}^{pl}$ is the
200 plastic component of the strain rate.

201 The average wall thicknesses of the inner and outer concrete core are 4.93 cm (1.94 inches)
202 and 11.43 cm (4.5 inches), respectively. The average thicknesses of the steel cylinder and mortar
203 coating are 0.15 cm (0.0598 inches) and 2.30 cm (0.904 inches), respectively. The center-to-
204 center spacing of prestressing wire wraps is set to be 1.10 cm (0.434 inches). The lengths of the
205 bell and spigot ends are considered to be 14 cm (5.5 inches) and 19.05 cm (7.25 inches),
206 respectively. The average wall thicknesses for the bell ring and spigot ring are 0.635 cm (0.25
207 inches) and 0.95 cm (0.375 inches), respectively. By virtue of symmetry, only half of each pipe
208 section is modeled with fixed displacement boundary condition in longitudinal direction
209 considered at the intact pipe side, thus allowing the damaged pipe to move in longitudinal
210 direction. In order to have a realistic behavior for the gasket joint, interface elements are used at
211 the joint to allow small movement to occur. An efficient approach developed by Mayer (2005) is
212 used to model the contact interfaces of joints with segment-to-segment contact elements like thin
213 layer or zero thickness elements used between spigot and bell ends.

214 The model was subjected to loads corresponding to internal fluid pressure, pipe and fluid
215 weights, and external earth loads as per the pipe dimensions and internal pressure and backfill
216 ratings defined by (AWWA C304-2007). The number of broken wire wraps was varied as shown
217 in Figure 4 in order to evaluate the cracking of the concrete core and the yielding of the

218 prestressing wires with increasing internal fluid pressure and number of broken wire wraps. The
219 lengths of damaged ECP sections corresponding to the various numbers of wire breaks
220 considered for the joint and the barrel are shown in Table 1. Three (3) different broken wire wrap
221 scenarios were modeled: starting from the spigot end and continuing along the pipe length,
222 starting from the bell end and continuing along the pipe length, and in the barrel of the pipe.

223 Figure 4. PCCP model with 5, 35, 70, and 100 broken wire wraps

224 Table 1. Damaged Pipe Length Corresponding to Number of Wire Breaks (WB)

225 **Material Properties**

226 The material properties used in the PCCP model are obtained from the current AWWA C304
227 - 2007. The concrete core is modeled with a 28-day compressive strength of 31 MPa (4,500 psi).
228 The Young's Modulus, density, and Poisson's Ratio used in the various components of the PCCP
229 model are shown in Table 2. The modulus of elasticity of the core concrete is calculated from
230 Equation 4 and modulus of elasticity of the mortar coating evaluated using Equation 5. The
231 stress-strain behavior of the concrete core and mortar coating are modeled based on the AWWA
232 C304 - 2007.

$$233 \quad E_c = (0.074)\gamma_c^{1.51} (f'_c)^{0.3} \quad (4)$$

$$234 \quad E_c = (0.074)\gamma_m^{1.51} (f'_m)^{0.3} \quad (5)$$

235 where γ_c is the concrete density, taken as 2,323 kg/m³ (145 lb/ft³); f'_c is the 28-day compressive
236 strength of concrete, taken as 31 MPa (4,500 psi); γ_m is the mortar coating density, considered as

237 2,242 kg/m³ (140 lb/ft³); and f'_m is the 28-day compressive strength of mortar coating, taken as
 238 37.9 MPa (5,500 psi).

239 Table 2. Material Properties of PCCP Based on AWWA C304 Standard

240 The gross wrapping stress, f_{sg} , which is the stress in the prestressing wire during wrapping, is
 241 considered as 75 percent of the specified minimum tensile strength of the wire, as shown in
 242 Equation 6. The yield strength of wire, f_{sy} , is taken as 85 percent of the specified tensile strength
 243 of the prestressing wire, as shown in Equation 7.

244
$$f_{sg} = (0.75)f_{su} \quad (6)$$

245
$$f_{sy} = (0.85)f_{su} \quad (7)$$

246 The prestressing wire used is a 6-gage, Class III wire, with an ultimate strength, f_u , of 1,737.5
 247 MPa (252 ksi). The Modulus of Elasticity of the wire, E_s , after wrapping at f_{sg} , for stress levels
 248 below f_{sg} is taken as 193,050 MPa (28,000 ksi). The stress-strain relationship for the prestressing
 249 wire, after wrapping at f_{sg} , is given in Equation 8.

250
$$f_s = \varepsilon_s E_s \quad \text{for } \varepsilon_s \leq f_{sg} / E_s$$

251
$$f_s = f_{su} \left(1 - [1 - 0.6133(\varepsilon_s E_s / f_{su})]^{2.25} \right) \quad \text{for } \varepsilon_s > f_{sg} / E_s \quad (8)$$

252 Where ε_s is strain in prestressing wire.

253 The yield strength of the steel cylinder in tension is taken as 227 MPa (33,000 psi), and the
 254 strength of the steel cylinder at failure is taken as 310 MPa (45,000 psi). Density and Poisson's
 255 Ratio of the prestressing wire and steel cylinder used in the model are shown in Table 2. The

256 compressive strength of the mortar coating, based on AWWA C304 standard, was 37.9 MPa
257 (5,500 psi) (AWWA C304-2007).

258 **Results and Discussion**

259 The effects of the location and number of broken wire wraps in a damaged PCCP with full
260 interaction at the gasket joint are evaluated by examining the stresses and strains developed in
261 various components of the pipe. Two main pipe failure indicators are considered: the onset of
262 micro and visible cracking in the concrete core and yielding and rupturing of the prestressed wire
263 wraps.

264 ***Cracking of Concrete Core***

265 Cracks are the first sign of deterioration in PCCP; micro cracks appear in the concrete at a
266 hoop strain of $2.0E-4$, while visible cracks appear at a hoop strain of $1.46E-2$. Once concrete in
267 tension begins to crack, its load carrying ability begins to decrease with additional strain. The
268 strain developed in the inside concrete core of the damaged ECP at the barrel of the pipe was
269 compared to the strain developed at the spigot and bell ends. Figure 12 shows an example
270 contour plot of the hoop strain in the concrete core of a PCCP with 70 wire breaks at the spigot
271 end when the internal fluid pressure reaches 862 kPa (125 psi). The results show that, under the
272 same level of damage, the hoop strain inside the concrete core at the invert of a Class 125-14
273 PCCP reaches the limits of micro cracking and visible cracking at much lower internal fluid
274 pressures when the damage occurs at the spigot end, compared with pipes having wire breaks at
275 the barrel and bell end of the pipe.

276 Figure 5. Hoop strain in concrete core of PCCP with 70 WB at spigot end with 862 kPa (125 psi)
277 internal pressure

278 ***Yield and Ultimate Strength of Prestressing Wires***

279 As additional internal fluid pressure loads are applied on a damaged PCCP with broken
280 prestressed wire wraps from corrosion or other causes listed earlier, the stress level in these wires
281 increases beyond the yield limit, and eventually the ultimate strength limit, thus leading to
282 additional wire breaks. This second failure indicator is investigated by monitoring the stresses in
283 prestressing wires in order to determine the internal fluid pressures which will cause them to
284 reach their yield and ultimate strength limits. The impact of growing number of broken
285 prestressing wire wraps on these stresses is also analyzed, and the results summarized in Table 3.
286 Figures 6 and 7 show the stress in the prestressing wires for PCCP with five (5) and thirty five
287 (35) broken wire wraps, respectively. Figures 8 and 9 show the stress in the prestressing wires
288 for PCCP with seventy (70) and hundred (100) broken wire wraps, respectively. Figures 6
289 through 9 compare the stresses in the prestressing wires when the damage occurs at various
290 locations of the PCCP: spigot end, bell end, and barrel.

291 Table 3. Internal Pressure Required to Yield or Rupture the Prestressing Wire Wraps

292 Figure 6. Stress in prestressing wires with five (5) broken wire wraps

293 Figure 7. Stress in prestressing wires with thirty-five (35) broken wire wraps

294 Figure 8. Stress in prestressing wires with seventy (70) broken wire wraps

295 Figure 9. Stress in prestressing wires with one hundred (100) broken wire wraps

296 It is clear from Figures 6 through 9 that when considering gasket-jointed ECP with full
297 joint interaction, the stress in the prestressing wire wraps reaches their yield limit at lower
298 internal fluid pressures when the wire breaks are at the spigot or bell end than when wire breaks
299 are at the barrel of the pipe. Figure 6 shows that for 5 wire breaks, yielding of the prestressing
300 wires occur at an internal fluid pressure of 1,979 kPa (287 psi) when the defect is at the barrel of
301 the pipe, compared to only 1,807 kPa (262 psi) when the defect is at the spigot end. In effect, the
302 internal fluid pressure that will result in yielding of the prestressed wires is 9% lower when the
303 defect is near the spigot end than when the defect is in the middle of the pipe. When considering
304 the complete rupture of the prestressing wires, this same difference becomes as much as 12.5%.

305 Figure 7 shows that the prestressing wire wraps of a PCCP with 35 wire breaks reach their
306 yield stress limit state at an internal fluid pressure that is 14.7% lower when the defect is at the
307 spigot end than when it is in the barrel of the pipe. This difference in internal pressure continues
308 to diverge until it reaches 16.3% at the ultimate (rupture) stress. The same can be said about
309 PCCP with 70 and 100 wire breaks where the yield-inducing internal pressures are 11% and 10%
310 lower at the spigot end, respectively, and the rupture-causing internal pressures are 11% and 13%
311 lower at the spigot end, as shown in Figures 8 and 9.

312 It can also be seen from the numbers of Table 3 and plots of Figures 6 through 9 that these
313 internal pressures that cause yielding and the eventual rupture of the wire wraps drop as the
314 number of respective wire breaks increase from 5 to 100. Figures 10 through 12 therefore,
315 compare—for each location of defect—how the internal pressure that causes failure of the
316 prestressing wires varies with the length of the defect, which corresponds to a different number
317 of broken wire wraps. When the wire breaks occur at the barrel of a PCCP, the prestressing wire
318 wraps reach their yield stress limit at internal fluid pressures of 1979 kPa (287 psi), 1310 kPa

319 (190 psi), 931 kPa (135 psi), and 731 kPa (106 psi) for 5, 35, 70, and 100 wire breaks,
320 respectively. Similarly, the onset of rupture for the prestressing wire wraps occurs at internal
321 fluid pressures of 1806 kPa (262 psi), 1117 kPa (162 psi), 827 kPa (120 psi), and 655 kPa (95
322 psi) for 5, 35, 70, and 100 wire breaks, respectively. These translate to a 63.5% drop in the
323 internal fluid pressure required to both yield or rupture the prestressing wires, as the defect
324 worsens from 5 to 100 wire breaks at the barrel of a PCCP. Similar numbers are obtained for
325 when the wire breaks occur at the bell end and the spigot end of the PCCP, as shown in Figures
326 11 and 12, respectively.

327 Figure 10. Stress in the prestressing wire –broken wire wraps in the barrel of the pipe

328 Figure 11. Stress in the prestressing wire –broken wire wraps at bell end

329 Figure 12. Stress in the prestressing wire –broken wire wraps at spigot end

330 **Conclusions and Recommendations**

331 In this paper, the effect of broken wire wraps on the structural performance of a damaged
332 PCCP was investigated using a three-dimensional numerical response model that accounted for
333 full interaction between the spigot and bell ends of adjacent pipes. A sensitivity analysis was
334 presented to give a better understanding of how the location and number of broken prestressing
335 wire wraps affect the failure pressure of the pipe. Three different locations of defects were
336 considered: spigot joint, bell joint, and barrel; as well as four different numbers of broken wire
337 wraps that varied from 5 to 100. The failure of the pipe was investigated by examining two
338 indicators: yielding of prestressed wire wraps in the vicinity of the damage and cracking of the
339 concrete core.

340 The results showed that wire wrap breaks at the joints— specifically the spigot joint—
341 decrease the overall pressure capacity of PCCP more so than wire breaks located at the barrel of
342 the pipe. The results indicate over 16% strength reduction for a low to medium number of wire
343 wrap breaks occurring at the spigot joint when compared to the barrel. In addition, the results
344 showed that if wire wrap breaks occur at the joint, it is anticipated that cracking in the pipe will
345 occur at much lower internal pressures than if the breaks occurred in the barrel of the pipe. These
346 internal pressure limits can also drop by as much as 65% with increased number of wire breaks.
347 It is therefore argued that the location and the number of broken prestressing wire wraps have a
348 significant effect on the structural performance of PCCP.

349 The results presented are significant for owners, operators, and inspectors of PCCP pipeline
350 systems alike. The conclusions arrived at will help these stakeholders better access the risk of
351 certain pipe defects for the purpose of more efficient and on-time replacement of these facilities.
352 While several issues regarding the structural performance of damaged PCCP with gasket joints
353 were discussed in this paper, there are many open questions and issues that need to be
354 researched. Future research into the structural performance and monitoring of PCCP should
355 include full-scale experimental models of PCCP as well as modeling PCCP with harnessed
356 joints.

357 **References**

- 358 1. Abi Shdid, C. and Hajali, M. (2014). “Detecting Location of Construction Defects in Drilled
359 Shafts Using Frequency Tomography Analysis of Cross-hole Sonic Logging.” *Proc. of the*
360 *2014 Int. Conf. of Computing in Civil and Building Engineering (ICCCBE)*, ASCE, Orlando,
361 FL, 1723-1730.
- 362 2. Alavinasab, A., Padewski E., Holley, M., Jha R., Ahmadi, G. (2010). “Damage Identification
363 Based on Vibration Response of Prestressed Concrete Pipes.” *Proc., Pipelines Conf.:*
364 *Climbing New Peaks to Infrastructure Reliability —Renew, Rehab, and Reinvest*, ASCE,
365 Keystone, CO, 909-919.
- 366 3. Alavinasab, A. and Hajali, M. (2014) “Do Broken Prestressing Wire Wraps at the joint
367 Affect the Safe Operation of a Pipe?.” *Pipelines 2014*: pp. 1379-1391.
368
- 369 4. Alavinasab, A., Padewski, E., Higgins, M. (2013). “Effects of the Location of Broken
370 Prestressing Wires Wraps in Structural Integrity of a Damaged PCCP.” *Proc., Pipelines*
371 *2013*, ASCE, Fort Worth, TX, 767-774.
372
373
- 374 5. Alavinasab, A., Padewski, E., Higgins, M., Holley, M., Jha, R., Ahmadi, G. (2011). “Crack
375 Propagation in Prestressed Concrete Noncylinder Pipe using Finite Element Method.” *Proc.,*
376 *Pipelines 2011: A Sound Conduit for Sharing Solutions*, ASCE, Seattle, WA, 55-64.
- 377 6. Alavinasab, A., Jha, R., Ahmadi, G. (2011). “Damage Identification based on Modal
378 Analysis of Prestressed Concrete Pipes.” *Proc., Pipelines 2011: A Sound Conduit for Sharing*
379 *Solutions*, ASCE, Seattle, WA, 12-23.
- 380 7. American Water Works Association (AWWA) (2007). “AWWA C301 Standard for
381 Prestressed Concrete Pressure Pipe, Steel-Cylinder Type.” Denver, CO.
- 382 8. American Water Works Association (AWWA) (2007). “AWWA C304 Design of Prestressed
383 Concrete Cylinder Pipe.” Denver, CO.
- 384 9. AWWA (2007), “AWWA C-304 Standard for Design of Prestressed Concrete Cylinder
385 Pipe.” Denver, CO.
386
- 387 10. AWWA Research Foundation (2007). “Failure of Prestressed Concrete Cylinder Pipe.”
388 Denver, CO.
389
- 390 11. Coghil, M. R. (2012). “Prestressed Concrete Cylinder Pipe Management: Communication
391 Methodologies and Decision Support Tools for the San Diego County Water Authority – a
392 Case Study.” *Proc., Pipelines 2013*, ASCE, Fort Worth, TX, 787-799.
393
- 394 12. Hajali, M. and Abi Shdid, C. (2013) “Determination of the two-dimensional plastic zone
395 shape and SIF at the crack tip using RKPM”. *Journal of Iron and Steel Research*, Elsevier,
396 20(12): pp. 103-114.
397

- 398 13. He, S., & Koizumi, A. (2012) “Damage Discrimination Analysis with Quantification Theory
399 for Sewage Pipe System”. *Journal of Pipeline Systems Engineering and Practice*, 4(1), 11-
400 16.
401
- 402 14. Kleiner, Y., Sadiq, R., & Rajani, B. (2004, August). “Modeling failure risk in buried pipes
403 using fuzzy Markov deterioration process”. *Proc., Int. Conf. on Pipeline Engineering and*
404 *Construction*, ASCE, San Diego, CA, 1-12.
405
- 406 15. Lee, J. and Fenves, G. L., (1998) “A plastic-damage model for cyclic loading of concrete
407 structures”. *Journal of Engineering Mechanics*, 124, 892-900.
408
- 409 16. Lubliner, J., Oliver, J., Oller, S. and Onate, E., (1989) “A plastic-damage model for
410 concrete”. *International Journal of Solids Structures*, 25(3), 299-326.
411
- 412 17. Mayer, M. H. and Gaul, L. (2005). “Segment-to-Segment Contact Elements for Modelling
413 Joint Interfaces in Finite Element Analysis.” *Mechanical Systems and Signal Processing*,
414 21(2), 724–734.
415
- 416 18. Najafi, M., Mielke, R., Ramirez, G., Keil, B., Davidenko, G., & Rahman, S. (2011). Analysis
417 and Testing of a Prototype Jointing System for Bar-Wrapped Steel Cylinder Concrete
418 Pressure Pipe. *ASCE Pipelines 2011: A Sound Conduit for Sharing Solutions*.
419
- 420 19. Nasser M. Amaitik and Saleh M. Amaitik (2008). “Development of PCCP Wire Breaks
421 Prediction Model Using Artificial Neural Networks.” *Proc., Pipelines 2008*, ASCE, Atlanta,
422 GA, 1-11.
423
- 424 20. Rauniyar, S. (2013). “Development of Finite Element Model for Analysis of Prestressed
425 Concrete Cylinder Pipe-embedded Cylinder Pipe with Experimental Comparison.” M.S.
426 thesis, The University of Texas at Arlington, Arlington, TX.
427
- 428 21. Selvakumar, A., Tuccillo, M. E., Martel, K. D., Matthews, J. C., & Feeney, C. (2013).
429 Demonstration and Evaluation of State-of-the-Art Wastewater Collection Systems Condition
430 Assessment Technologies. *Journal of Pipeline Systems Engineering and Practice*, 5(2).
431
- 432 22. Wilson, J. F. (2011). Failure Analysis of a Buried Pipeline Transporting Gas. *Journal of*
433 *Pipeline Systems Engineering and Practice*, 3(1), 17-21.
434
435
- 436 23. Xiong, H., Li, P., and Lia, Q. (2010). “FE model for simulating wire-wrapping during
437 prestressing of an embedded prestressed concrete cylinder pipe.” *Simul. Model. Prac. Theo.*
438 18(5), 624-636.

439

440

441 **Table 1.** Damaged Pipe Length Corresponding to Number of Wire Breaks (WB)

ECP Designation	Class	Internal Pressure Rating	Backfill Height Rating	Damage Length, cm (inches)			
				5 WB	35 WB	70 WB	100 WB
Class 125-14		0.86 MPa (125 psi)	4.3 m (14 ft)	5.5 (2.17)	38.6 (15.18)	77.2 (30.36)	110.2 (43.38)

442

443 **Table 2.** Material Properties of PCCP Based on AWWA C304 Standard

	Young's Modulus (GPa) / (psi)	Density (kg/m ³) / (lb/ft ³)	Poisson's ratio
Concrete	27.17 / 3.94E6	2,322.61 / 145	0.2
Mortar Coating	25.1 / 3.64E6	2,242.58 / 140	0.2
Prestressing Wires	193.05 / 28E6	7,832.8 / 489	0.3
Steel Cylinder	206.84 / 3E7	7,832.8 / 489	0.3

444

445 **Table 3.** Internal Pressure Required to Yield or Rupture the Prestressing Wire Wraps

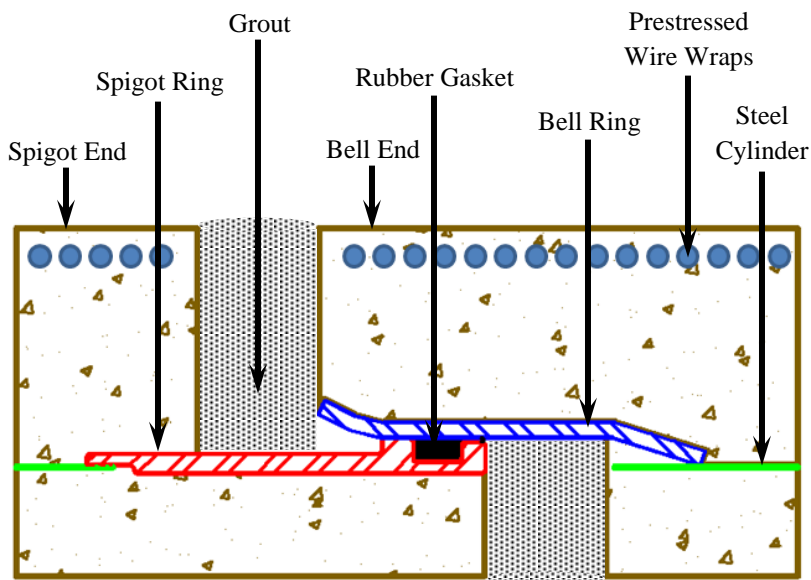
Number of Broken Wire Wraps	Yield (kPa) / (psi)			Rupture (kPa) / (psi)		
	Barrel	Spigot	Bell	Barrel	Spigot	Bell
5	1979/287	1806/262	1896/275	2344/340	2055/298	2137/310
35	1310/190	1117/162	1200/174	1482/215	1241/180	1331/193
70	931/135	827/120	883/128	1000/145	889/129	938/136
100	731/106	655/95	703/102	793/115	689/100	745/108

446

447

448

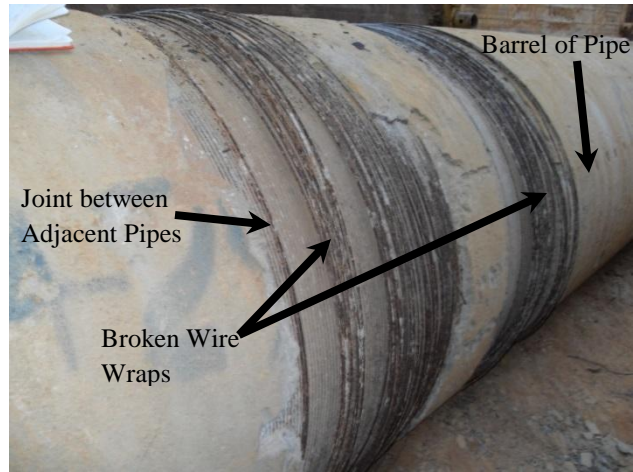
449



450

451
452

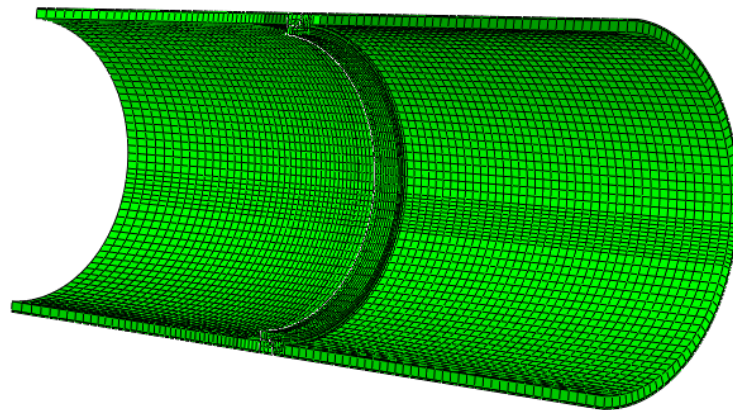
Fig 1. Schematic of the joint in PCCP



453

Fig 2. Broken wire wraps at different locations in PCCP

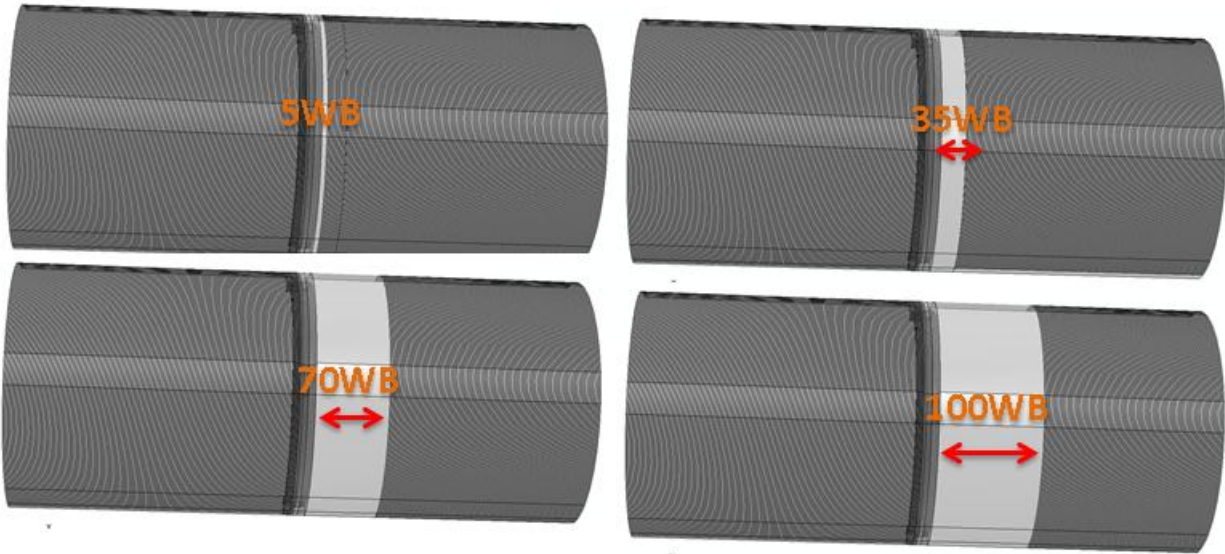
454
455
456



457

Fig 3. Spigot and bell ends of the PCCP numerical model

458
459
460

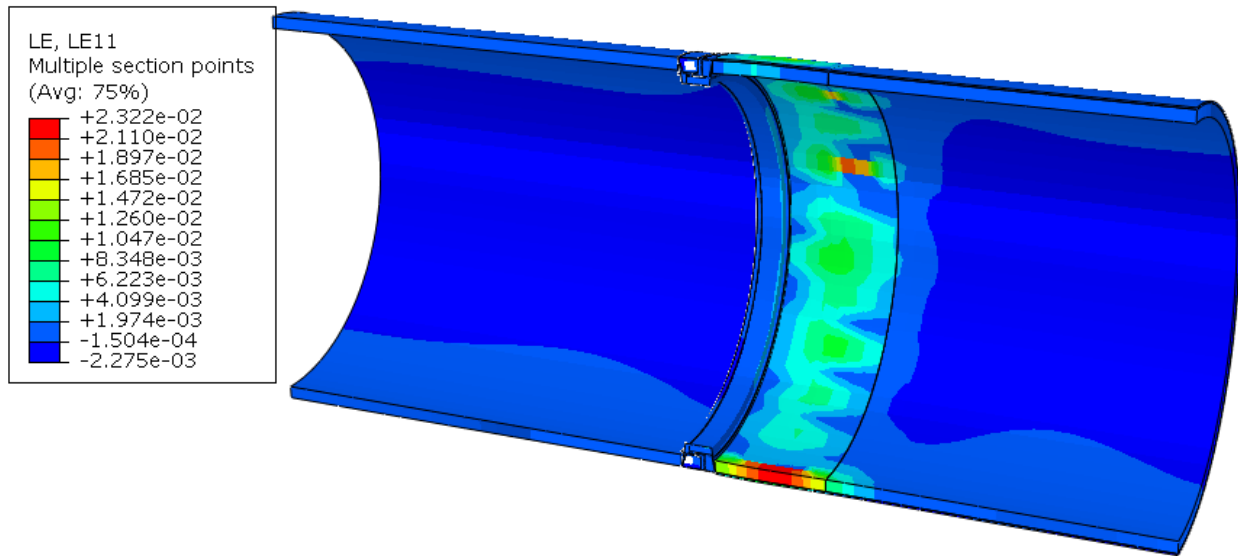


461

462

463

Figure 4. PCCP model with 5, 35, 70, and 100 broken wire wraps



464

465

466

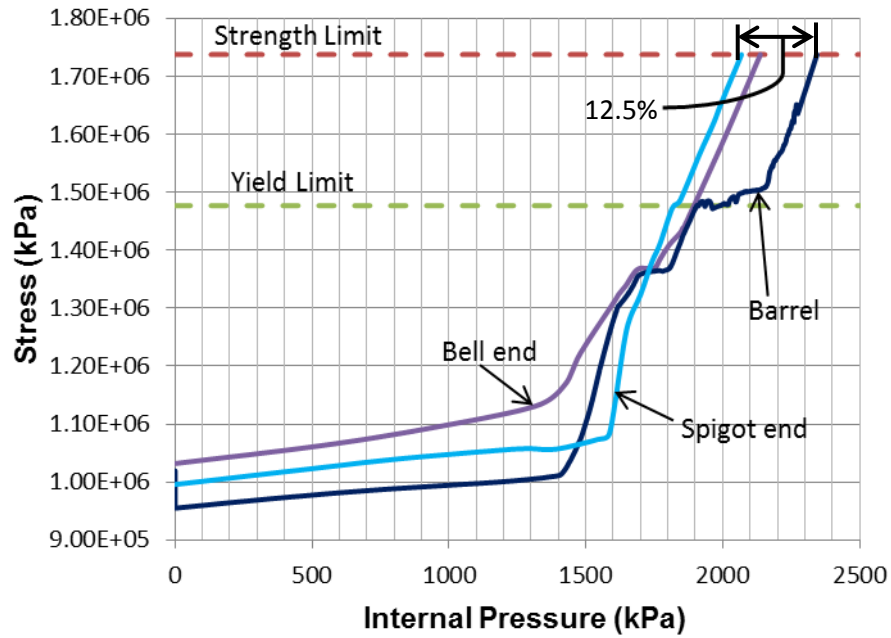
467

Fig 5. Hoop strain in concrete core of PCCP with 70 WB at spigot end with 862 kPa (125 psi) internal pressure

468

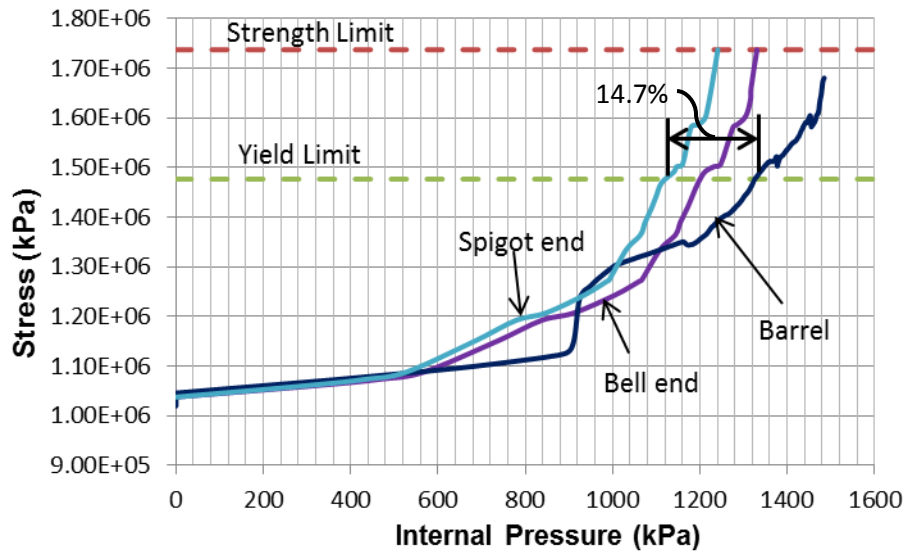
469

470



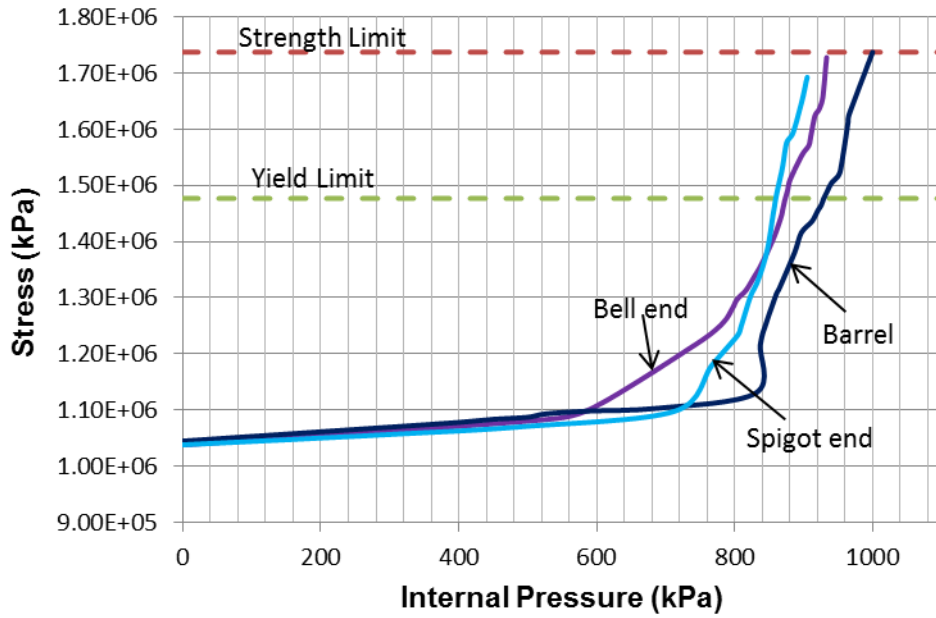
471
472
473

Fig 6. Stress in prestressing wires with five (5) broken wire wraps



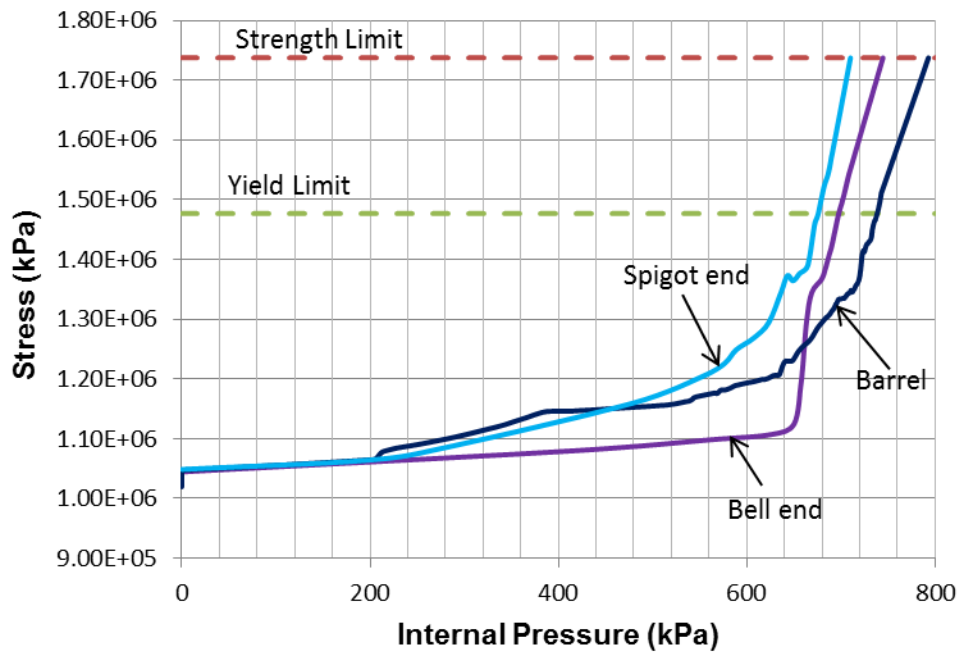
474
475

Fig 7. Stress in prestressing wires with thirty-five (35) broken wire wraps



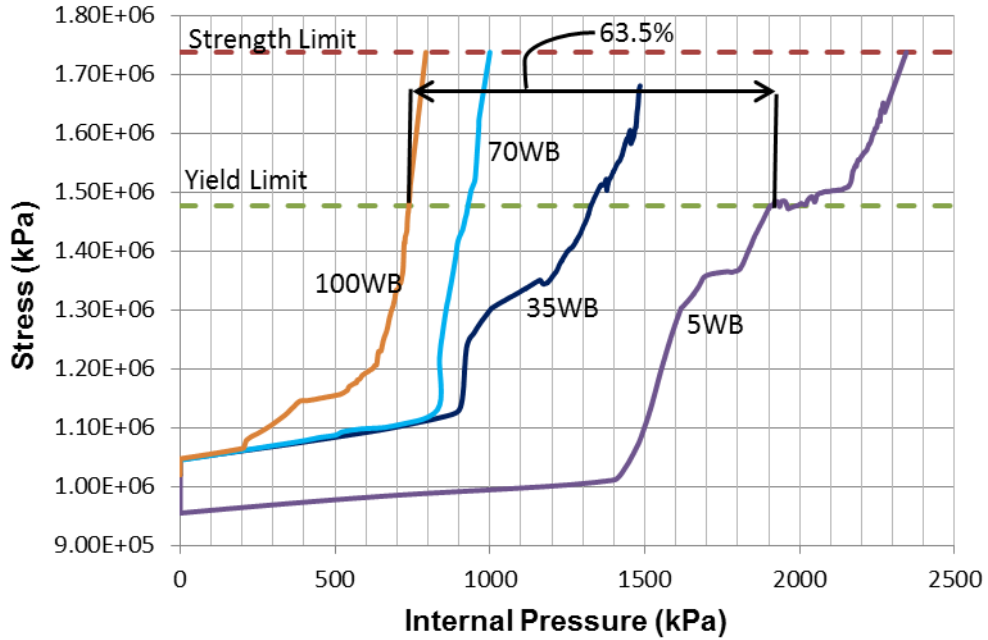
476
477
478

Fig 8. Stress in prestressing wires with seventy (70) broken wire wraps



479
480
481
482
483
484

Fig 9. Stress in prestressing wires with one hundred (100) broken wire wraps

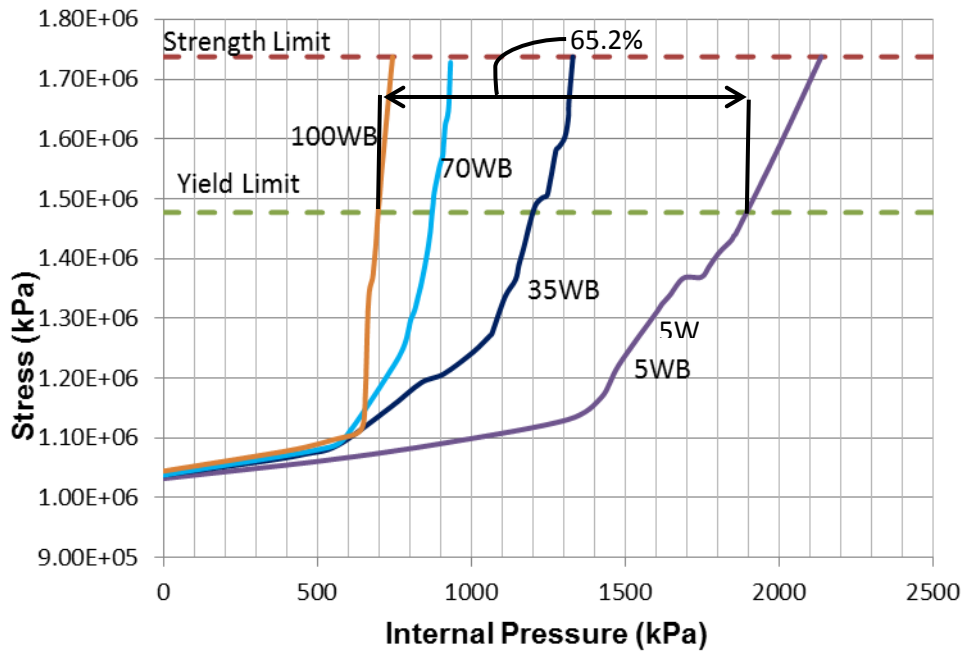


485

486

Fig 10. Stress in the prestressing wire –broken wire wraps in the barrel of the pipe

487

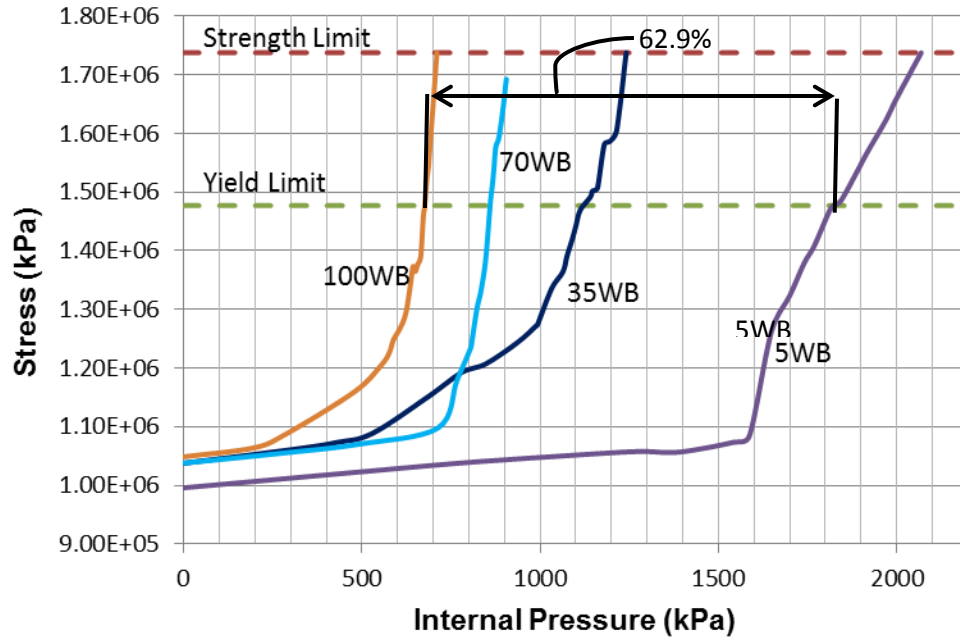


488

489

Fig 11. Stress in the prestressing wire –broken wire wraps at bell end

490



491

492

Fig 12. Stress in the prestressing wire –broken wire wraps at spigot end

493

494

495

496

1 Table 1. Damaged Pipe Length Corresponding to Number of Wire Breaks (WB)

ECP Designation	Class	Internal Pressure Rating	Backfill Height Rating	Damage Length, cm (inches)			
				5 WB	35 WB	70 WB	100 WB
Class 125-14		0.86 MPa (125 psi)	4.3 m (14 ft)	5.5 (2.17)	38.6 (15.18)	77.2 (30.36)	110.2 (43.38)

2

3 Table 2. Material Properties of PCCP Based on AWWA C304 Standard

	Young's Modulus (GPa) / (psi)	Density (kg/m ³) / (lb/ft ³)	Poisson's ratio
Concrete	27.17 / 3.94E6	2,322.61 / 145	0.2
Mortar Coating	25.1 / 3.64E6	2,242.58 / 140	0.2
Prestressing Wires	193.05 / 28E6	7,832.8 / 489	0.3
Steel Cylinder	206.84 / 3E7	7,832.8 / 489	0.3

4

5 Table 3. Internal Pressure Required to Yield or Rupture the Prestressing Wire Wraps

Number of Broken Wire Wraps	Yield (kPa) / (psi)			Rupture (kPa) / (psi)		
	Barrel	Spigot	Bell	Barrel	Spigot	Bell
5	1979/287	1806/262	1896/275	2344/340	2055/298	2137/310
35	1310/190	1117/162	1200/174	1482/215	1241/180	1331/193
70	931/135	827/120	883/128	1000/145	889/129	938/136
100	731/106	655/95	703/102	793/115	689/100	745/108

6

1
2
3
4
5
6
7
8
9
10

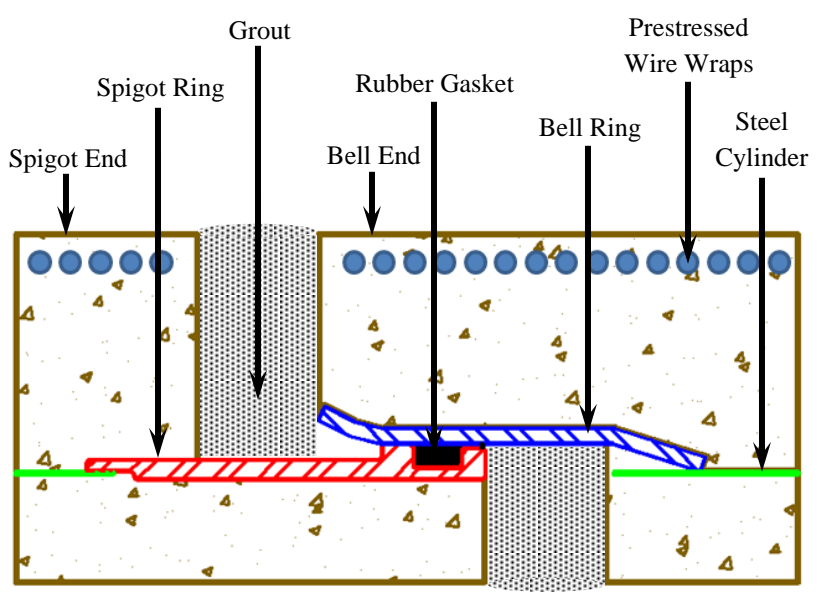


Figure 1. Schematic of the joint in PCCP

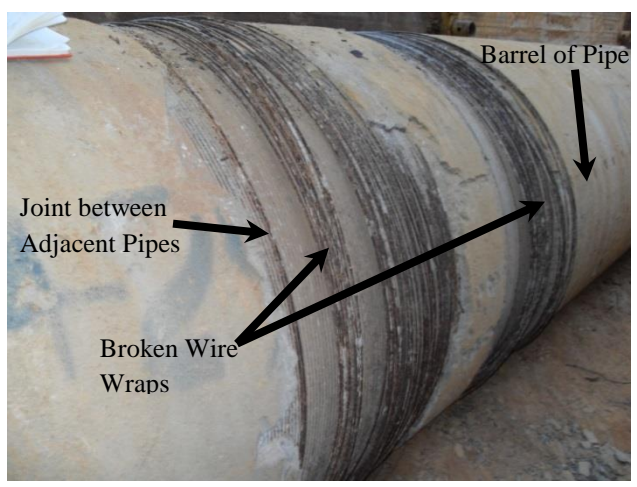
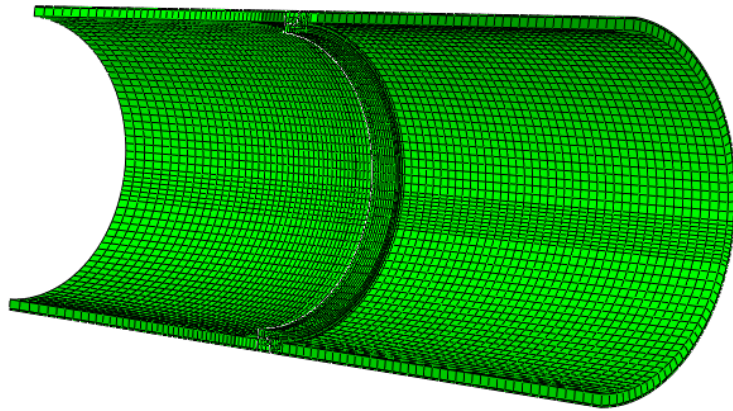


Figure 2. Broken wire wraps at different locations in PCCP



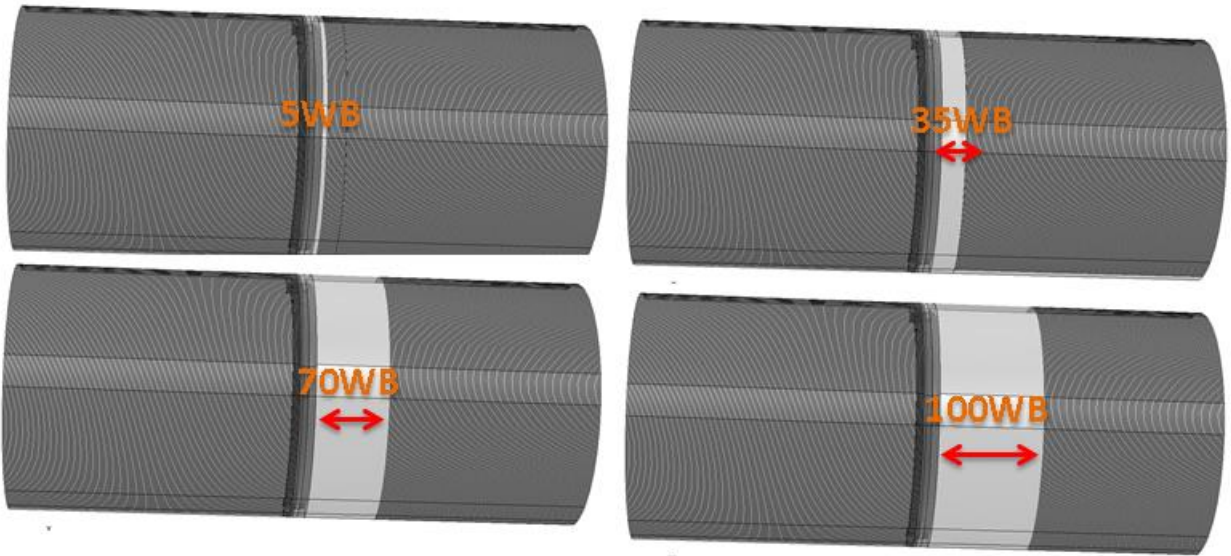
11

12

13

14

Figure 3. Spigot and bell ends of the PCCP numerical model

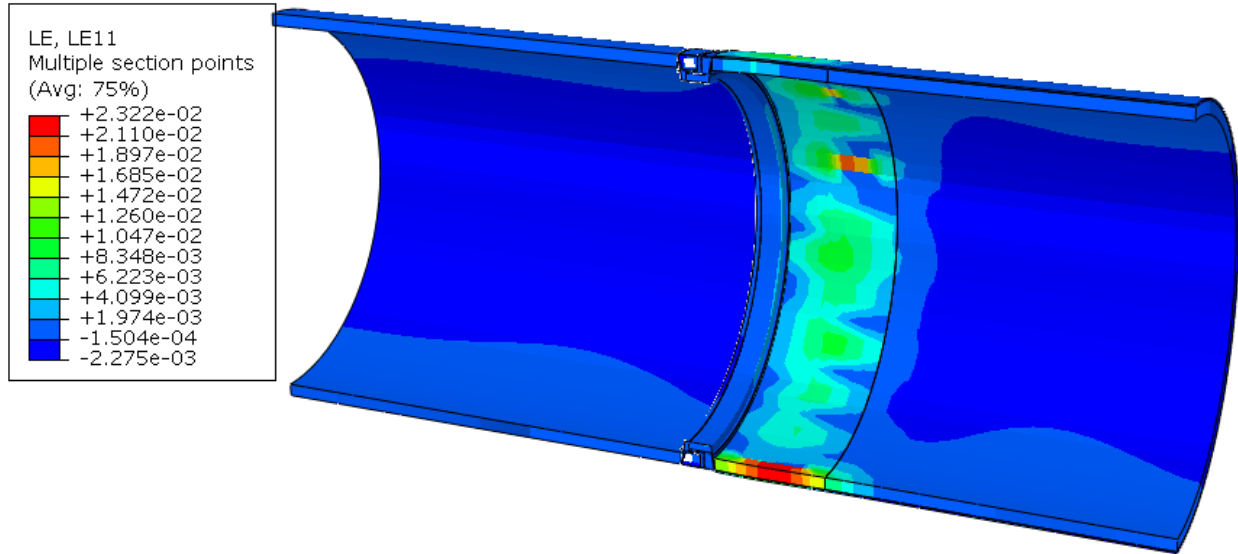


15

16

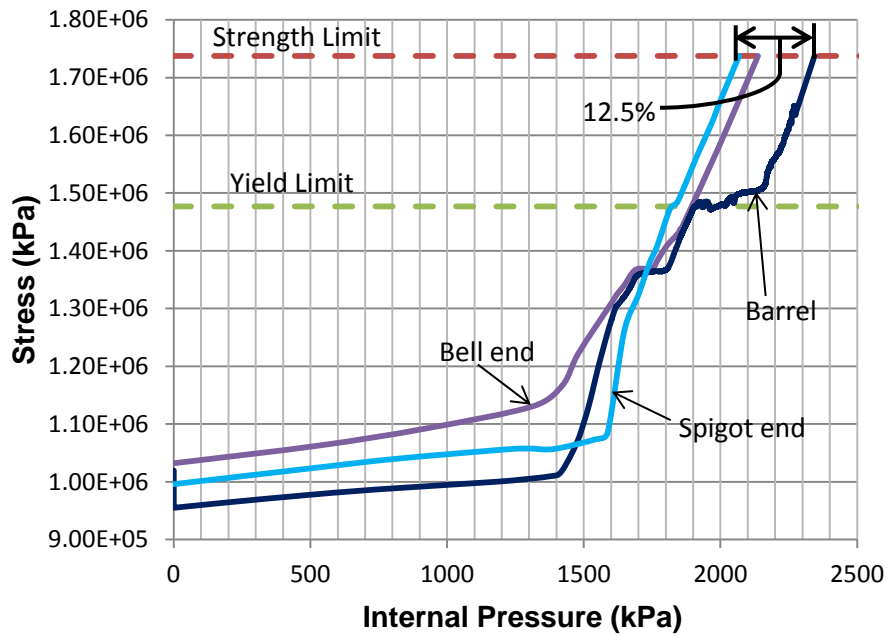
17

Figure 4. PCCP model with 5, 35, 70, and 100 broken wire wraps

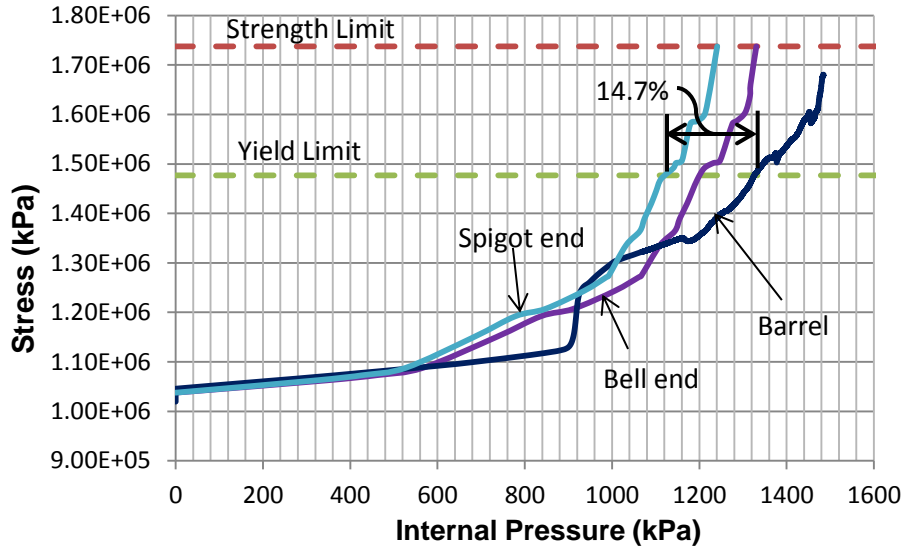


18
19 Figure 5. Hoop strain in concrete core of PCCP with 70 WB at spigot end with 862 kPa (125 psi)
20 internal pressure
21

22
23
24

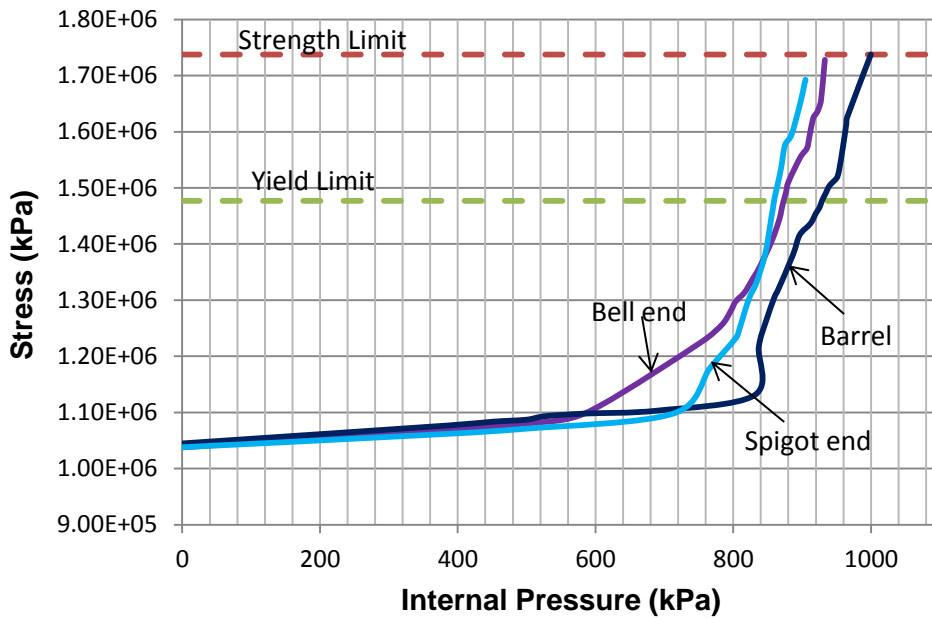


25
26 Figure 6. Stress in prestressing wires with five (5) broken wire wraps
27



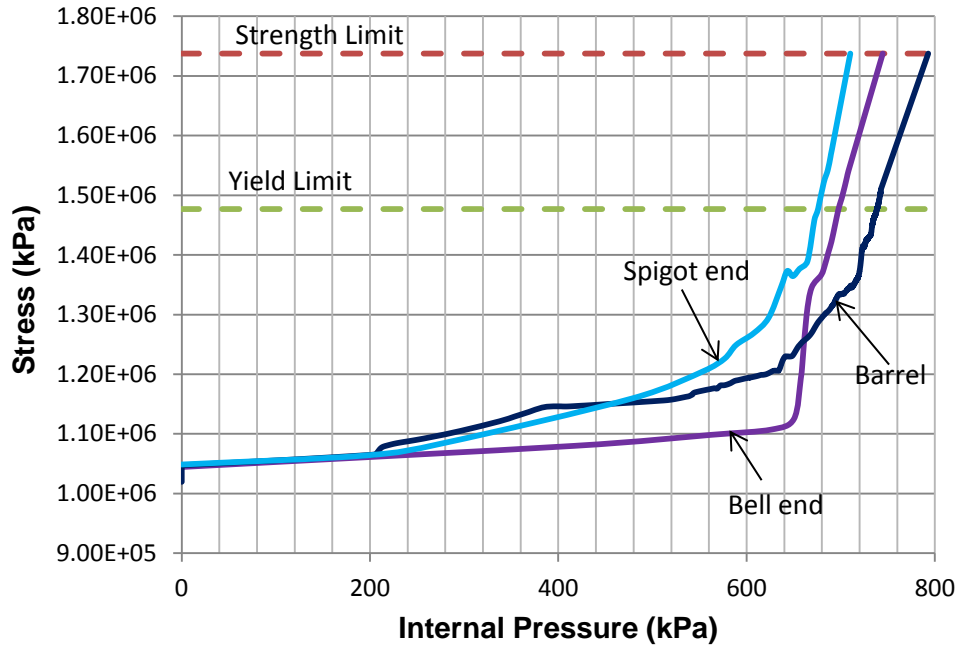
28
29

Figure 7. Stress in prestressing wires with thirty-five (35) broken wire wraps



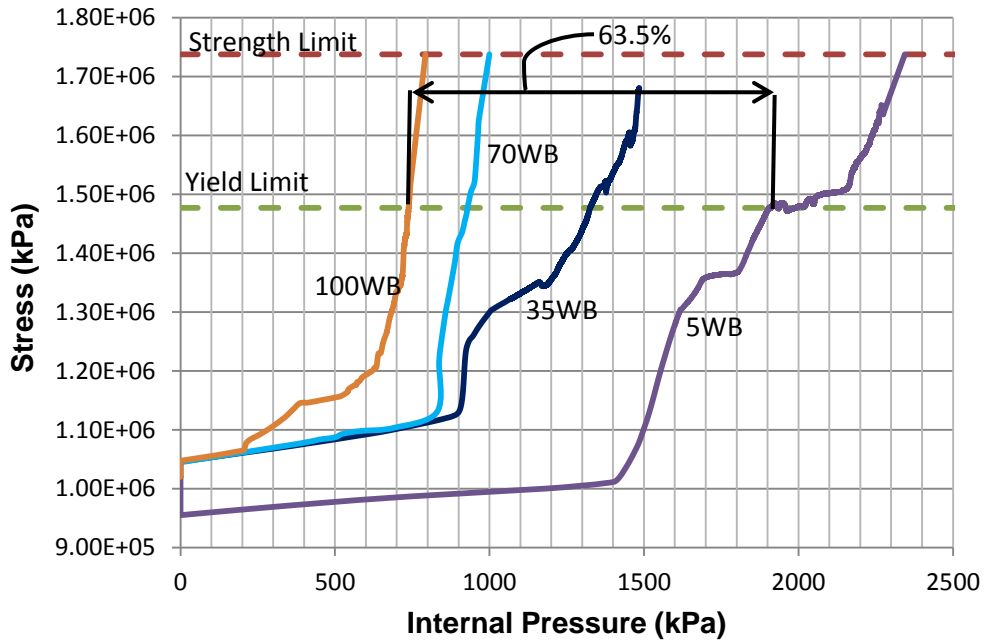
30
31
32

Figure 8. Stress in prestressing wires with seventy (70) broken wire wraps



33
34
35
36
37
38

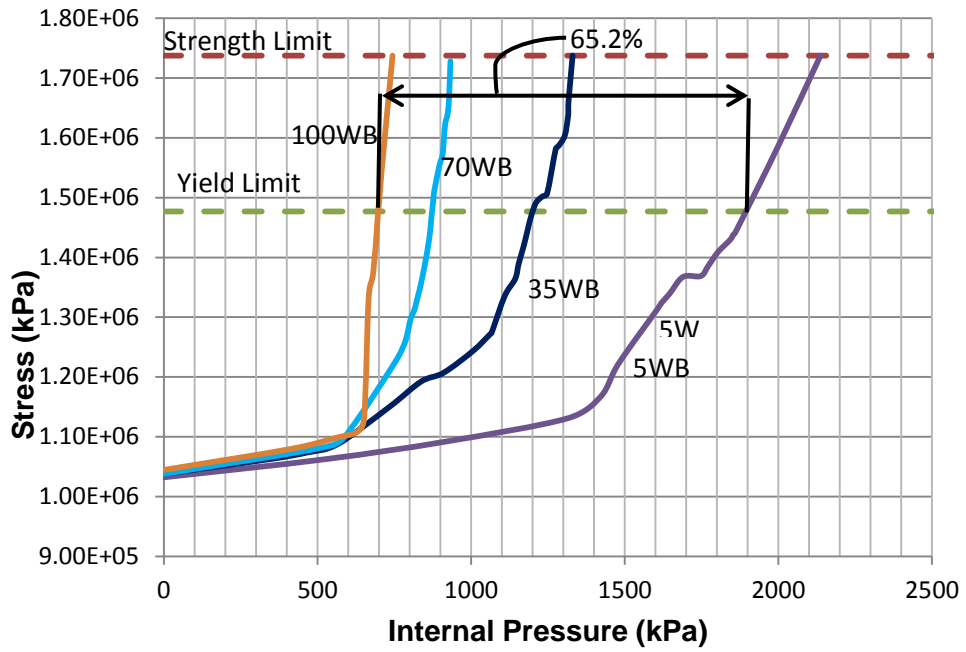
Figure 9. Stress in prestressing wires with one hundred (100) broken wire wraps



39
40

Figure 10. Stress in the prestressing wire –broken wire wraps in the barrel of the pipe

41

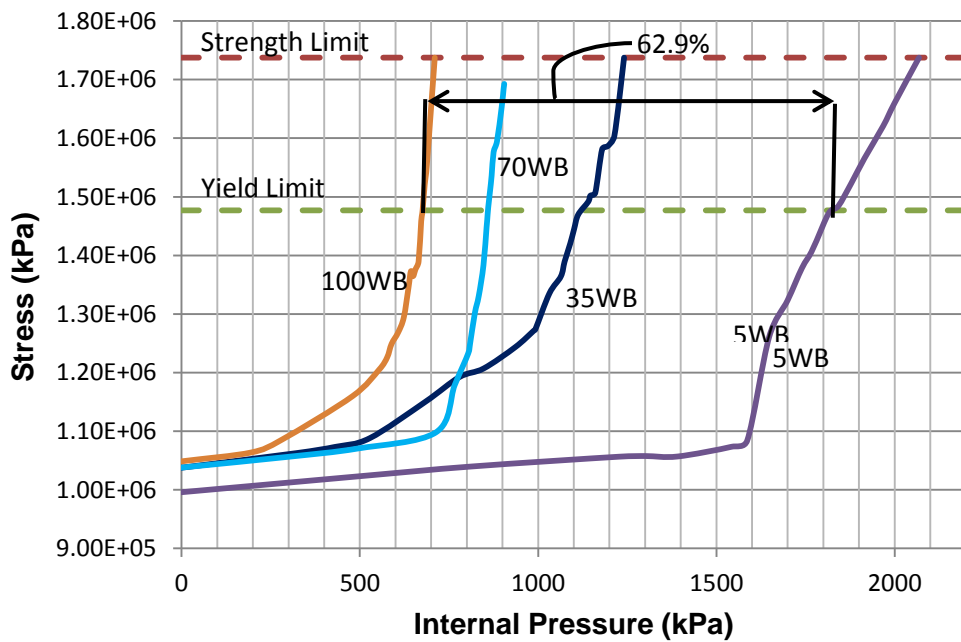


42

43

Figure 11. Stress in the prestressing wire –broken wire wraps at bell end

44



45

46

Figure 12. Stress in the prestressing wire –broken wire wraps at spigot end

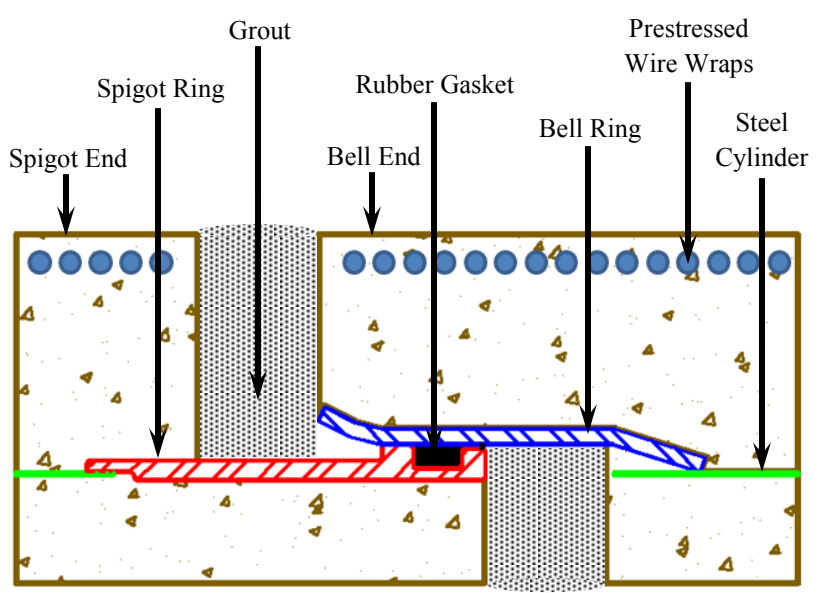


Fig 1. Schematic of the joint in PCCP

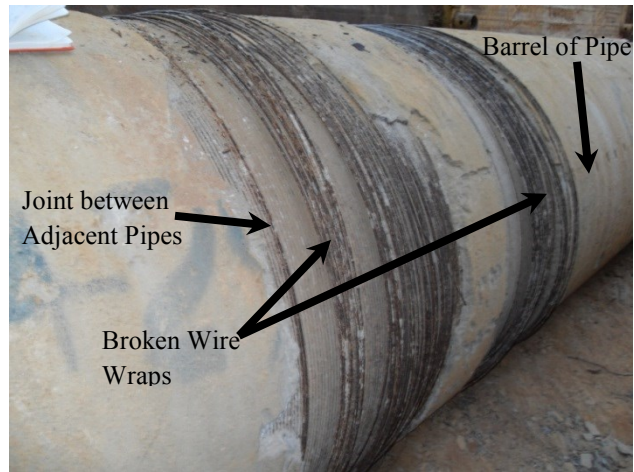


Fig 2. Broken wire wraps at different locations in PCCP

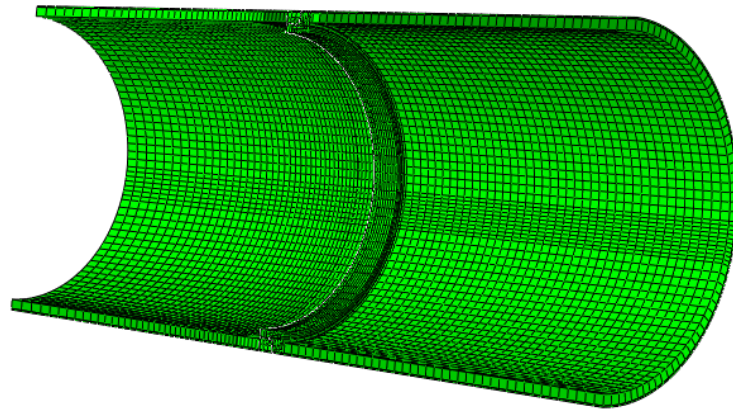


Fig 3. Spigot and bell ends of the PCCP numerical model

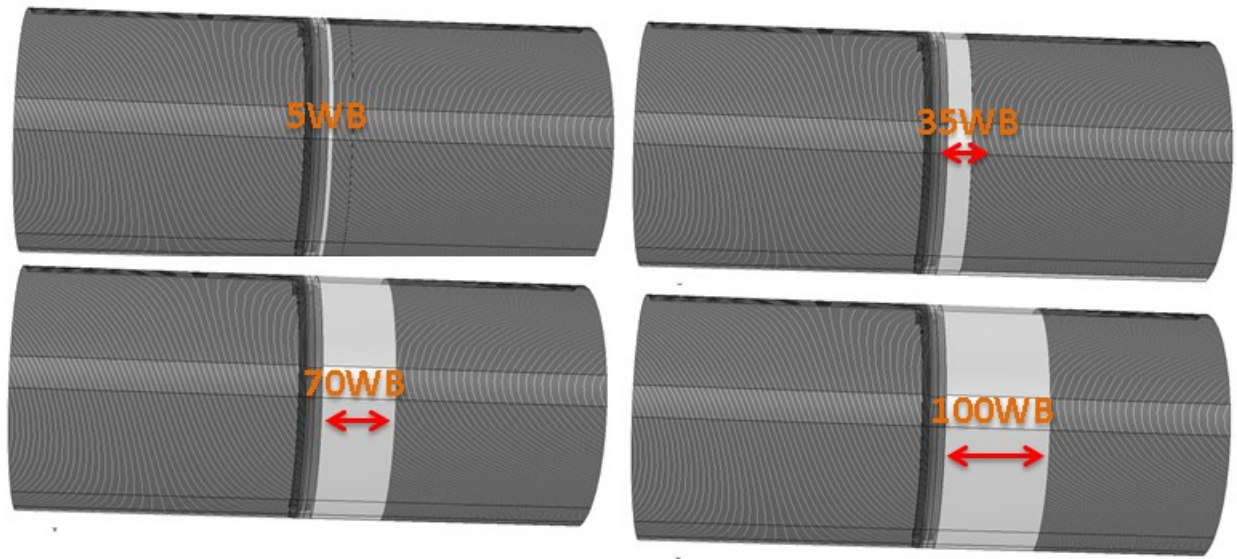


Figure 4. PCCP model with 5, 35, 70, and 100 broken wire wraps

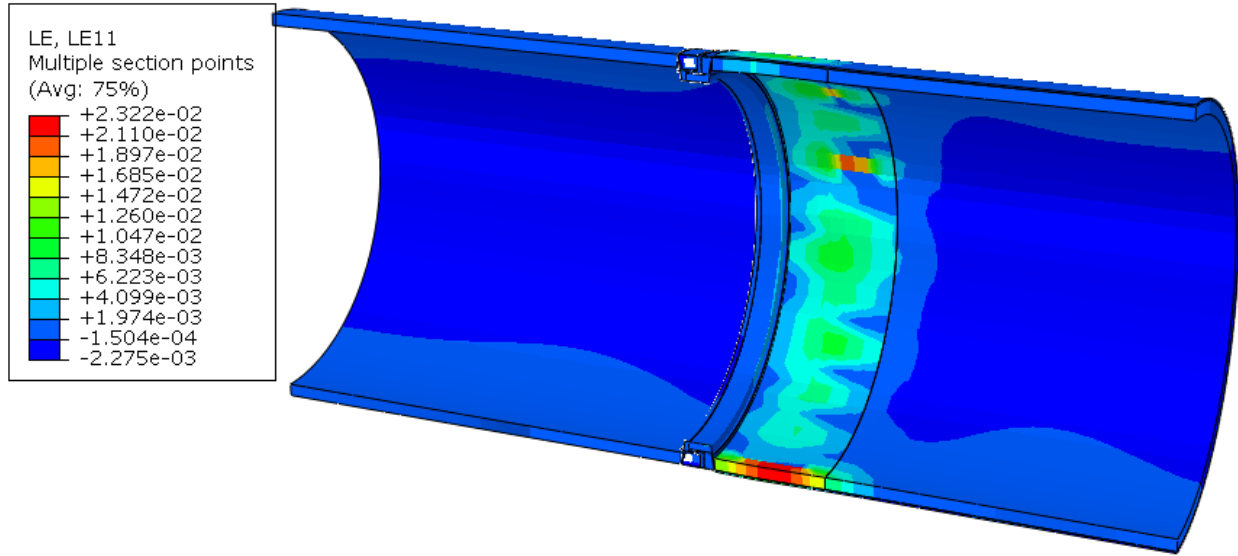


Fig 5. Hoop strain in concrete core of PCCP with 70 WB at spigot end with 862 kPa (125 psi) internal pressure

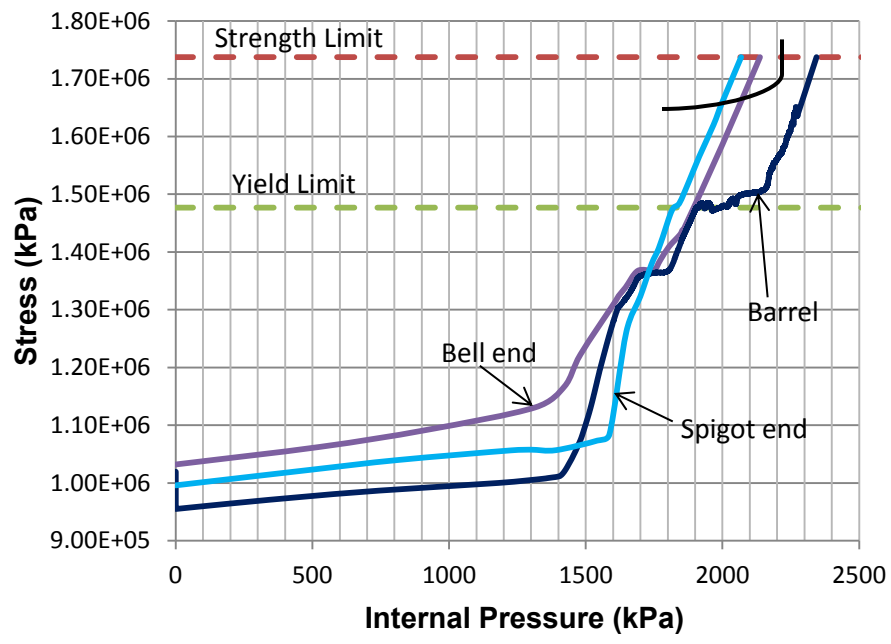


Fig 6. Stress in prestressing wires with five (5) broken wire wraps

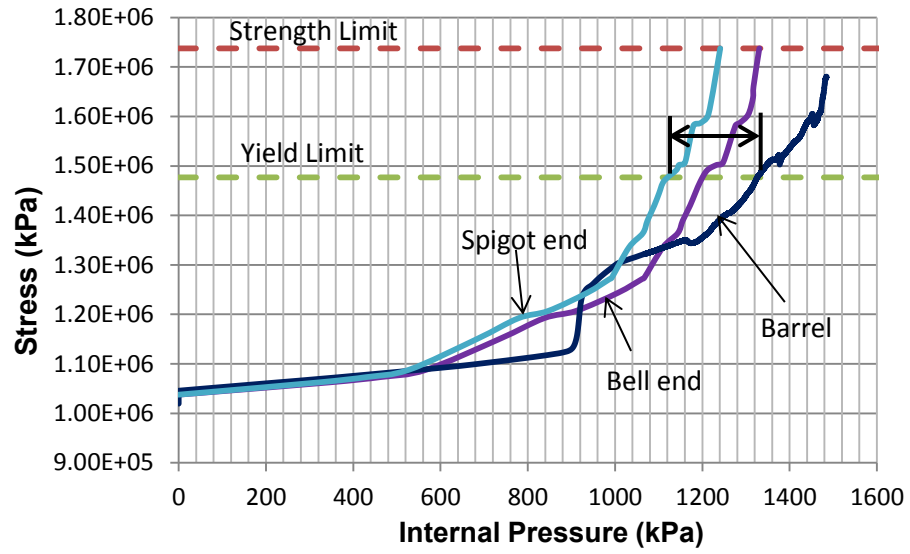


Fig 7. Stress in prestressing wires with thirty-five (35) broken wire wraps

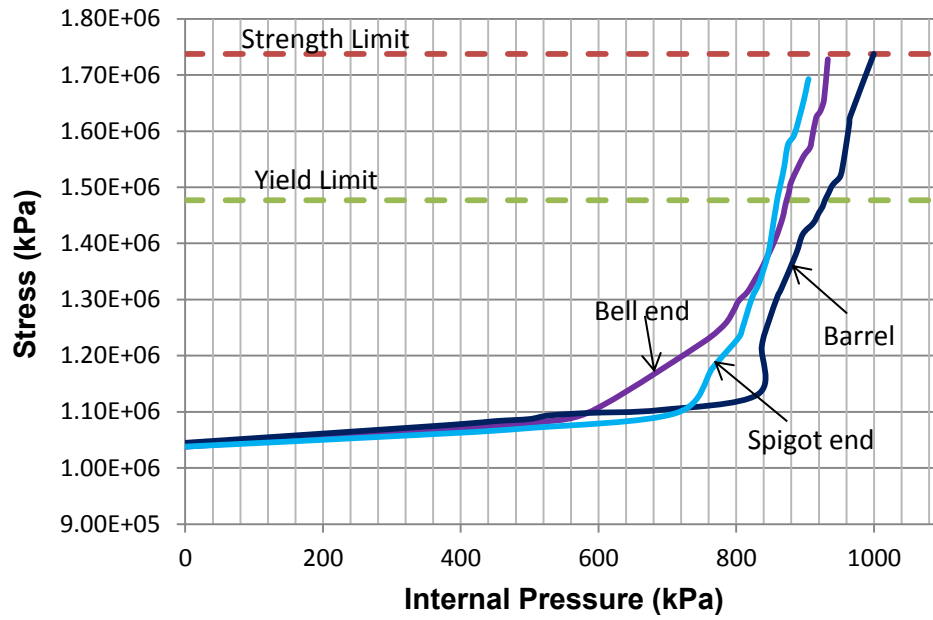


Fig 8. Stress in prestressing wires with seventy (70) broken wire wraps

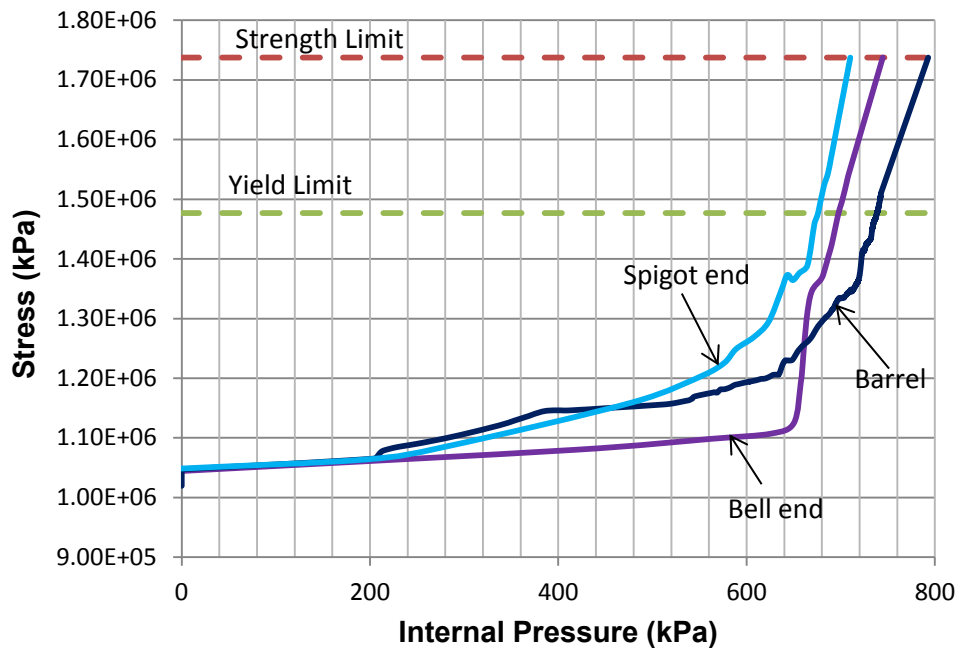


Fig 9. Stress in prestressing wires with one hundred (100) broken wire wraps

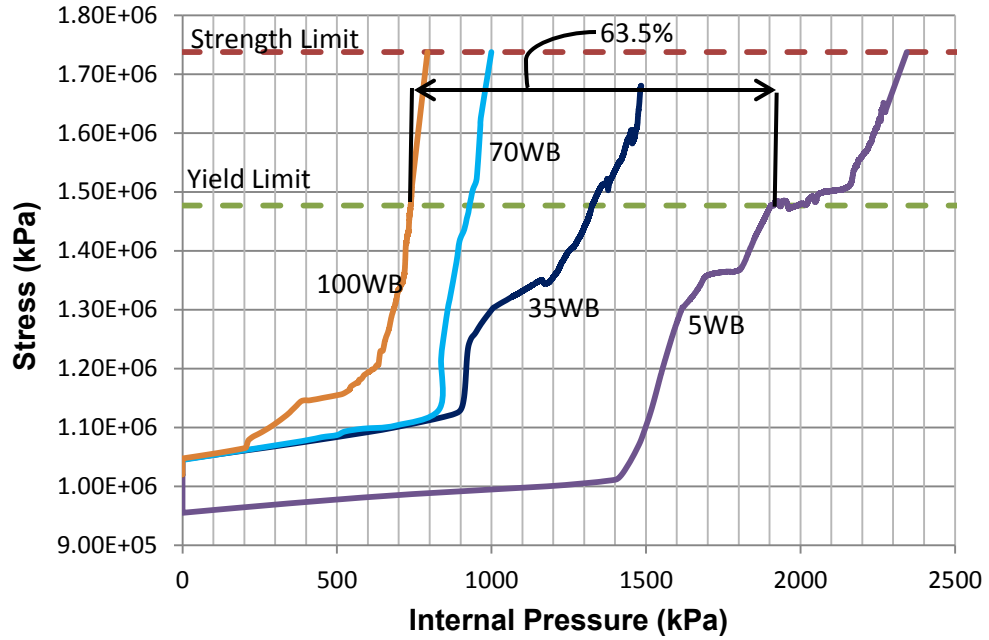


Fig 10. Stress in the prestressing wire –broken wire wraps in the barrel of the pipe

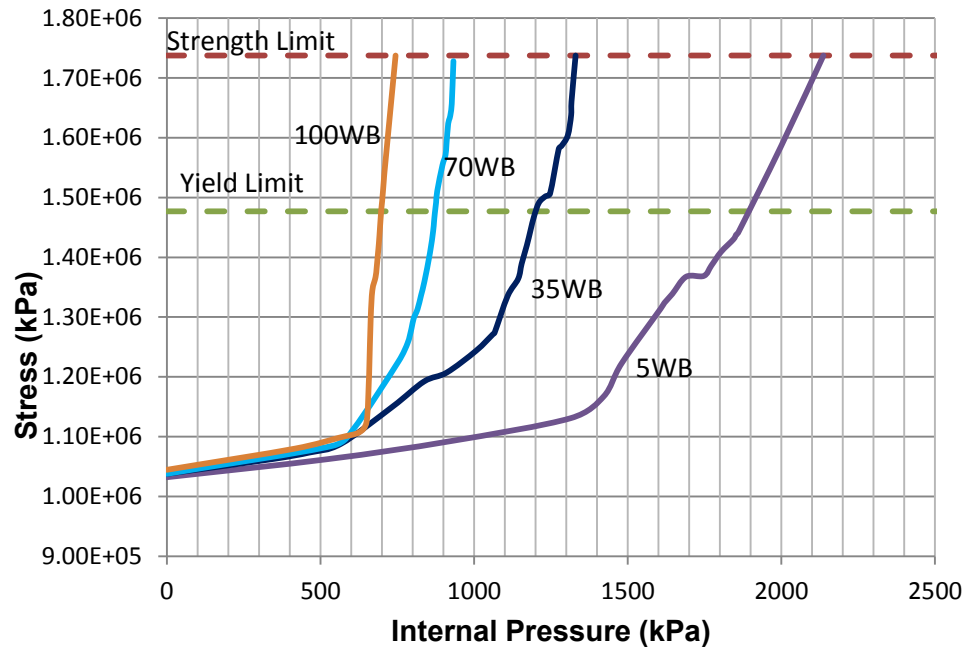


Fig 11. Stress in the prestressing wire –broken wire wraps at bell end

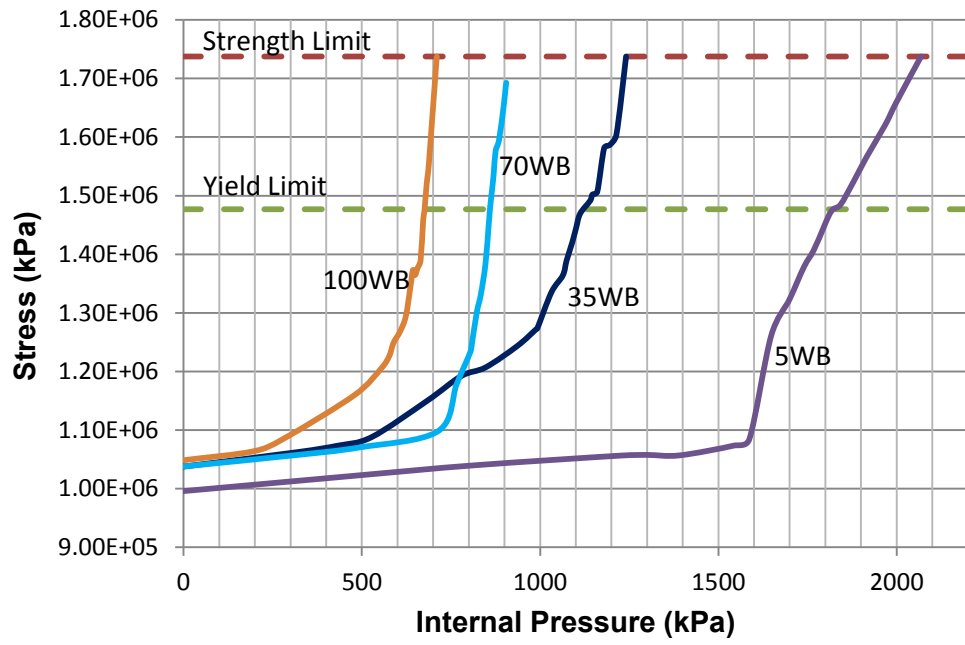


Fig 12. Stress in the prestressing wire –broken wire wraps at spigot end

Fig 1. Schematic of the joint in PCCP

Fig 2. Broken wire wraps at different locations in PCCP

Fig 3. Spigot and bell ends of the PCCP numerical model

Fig 4. PCCP model with 5, 35, 70, and 100 broken wire wraps

Fig 5. Hoop strain in concrete core of PCCP with 70 WB at spigot end with 862 kPa (125 psi) internal pressure

Fig 6. Stress in prestressing wires with five (5) broken wire wraps

Fig 7. Stress in prestressing wires with thirty-five (35) broken wire wraps

Fig 8. Stress in prestressing wires with seventy (70) broken wire wraps

Fig 9. Stress in prestressing wires with one hundred (100) broken wire wraps

Fig 10. Stress in the prestressing wire –broken wire wraps in the barrel of the pipe

Fig 11. Stress in the prestressing wire –broken wire wraps at bell end

Fig 12. Stress in the prestressing wire –broken wire wraps at spigot end